LORENTZ CONTRACTED GEOMETRICAL MODEL*

A.D. KRISCH
Randall Laboratory of Physics, University of Michigan, Ann Arbor, Michigan 48104, USA

Received 12 January 1973

The model assumes that when two high energy particles collide each behaves as a geometrical object which has a Gaussian density and is spherically symmetric except for the Lorentz-contraction in the incident direction. Folding the two spatial distribution together we obtain the slope (b) of the elastic diffraction peak in terms of the c.m. velocities (β_i and β_j) and the sizes (A_i and A_j) of the two incident particles. These sizes are assumed to have the experimental s-dependence of $\sigma_{\text{tot}} \propto \pi A^2$ for each reaction. The combined s-dependence of the σ_{tot}'s and the β's gives the s-dependence of the elastic slope $b_{ij}(s) = \frac{1}{2}(A_i^2\beta_i^2 + A_j^2\beta_j^2)\,\sigma_{\text{tot}}^{ij}(s)/\sigma_{\text{tot}}^{ij}(\infty)$. This formula agrees with the experimental slope for p–p, $\bar{\text{p}}$–p, K^+–p, K^-–p and $\pi^\pm$–p elastic scattering from 3 to 1500 GeV/c, with only 3 parameters: $A_\pi^2 = 6.1$, $A_\text{K}^2 = 3.3$ and $A_\text{p}^2 = 10.5\ (\text{GeV}/c)^{-2}$.

Recently ISR results on elastic [1] and inclusive [2] scattering have renewed interest in geometrical models for high energy proton-proton scattering. Such model have been studied for the last 10 years even though they are never completely fashionable. Serber's [3] optical model for elastic scattering was probably the first geometrical model, and it was soon followed by the models of Krisch [4], Van Hove [5], Wu and Yang [6] and others. Models with at least some geometrical aspects have been applied to inclusive reactions by Van Hove [5], Krisch [7–9], Hung [10], Yang et al. [11], Feynman [12] and others.

A nice feature of geometrical models is that they led to some predictions for very high energy cross sections which now seem supported by ISR data. Yang et al. [11] predicted that inclusive cross sections would approach a limit using a model that is at least partially geometrical. Feynman [12] predicted that the inclusive pion production cross section $E\,\mathrm{d}^3\sigma/\mathrm{d}P^3$ would be s-independent when plotted against X and $P_\perp$. The variable X, which is a vital part of Feynman's model, was essentially suggested earlier by Huang [10] using the Lorentz-contracted geometrical model [7, 8]; and Feynman's model itself seems partially geometrical. ISR data indicate that indeed $E\,\mathrm{d}^3\sigma/\mathrm{d}P^3$ is s-independent for $X > 0.1$ from 12 to 1500 GeV/c^2. These predictions of geometrical models for inclusive reactions were recently discussed [9] and we will not stress them here.

The Lorentz-contracted geometrical model also predicted that the shrinkage of the p–p elastic diffraction peak would disappear ar ISR energies. Krisch [8] suggested that the elastic cross section should depend only on $\beta^2P_\perp^2$; therefore the slope b in an e^{bt} plot should be proportional to β^2, the square of the c.m. velocity of each proton. In fact he predicted that the pp cross section should have the form:

$$\frac{\mathrm{d}\sigma\dagger}{\mathrm{d}t}\left[\frac{\text{mb}}{(\text{GeV}/c)^2}\right] = 90\exp(-10\beta^2P_\perp^2) + 0.74\exp(-3.45\beta^2P_\perp^2) + 0.0029\exp(-1.45\beta^2P_\perp^2)\,. \tag{1}$$

Recently Leader and Pennington [13] and others [14] showed that in the diffraction peak this preduction was verified by the ISR data. They also introduced a new variable n^2 that is mathematically equal to $\beta^2P_\perp^2$ for p–p scattering, but has a group theoretic rather than geometrical origin.

Eq. (1) also predicted the large $\beta^2P_\perp^2$ behavior of high energy elastic scattering. The † refers to particle identity effects near 90° which depend on the spin-dependence of p–p scattering which remains to be studied. Some deviations [15, 16] have been found in the range $\beta^2P_\perp^2 = 1 \to 4(\text{GeV}/c)^2$. In fact it now

* Supported by a research grant from the U.S. Atomic Energy Commission.

appears that the 2nd region of this "onion" model may disappear at very high energy; recent ISR data [17] in this $\beta^2 P_\perp^2$ range appears to lie almost on the $\exp(-1.45\beta^2 P_\perp^2)$ line. But the ISR data have large errors and we must await more precise data from the ISR and NAL to settle the large $\beta^2 P_\perp^2$ behavior. We will concentrate here on the elastic diffraction peak where there is precise data up to 1500 GeV/c [1, 18]. The model did not predict the newly discovered forward peak $[P_\perp^2 < 0.1(\mathrm{GeV}/c)^2]$ which may be another region of the onion. However as will be shown later, the s-dependence of the slope is also proportional to β^2 in this region [9]. Nevertheless we will concentrate on the region $0.1 < P_\perp^2 < 0.5$ $[\mathrm{GeV}/c]^2$ where the data are most complete.

In our earlier papers [8] we did not satisfactorially treat the case of unlike particles. We did plot the πp elastic cross section against $\beta^2 P_\perp^2$ and found a good fit; however we were arbitrary [19] in using the β_{cm} of the pion rather than the proton. Moreover, we suggested the the s-dependence of $\sigma_{\mathrm{tot}}(\mathrm{p{-}p})$ was responsible for the anti-shrinkage of the $\bar{\mathrm{p}}$–p slope; but we ignored the non-negligible s-dependence of $\sigma_{\mathrm{tot}}(\pi{-}\mathrm{p})$ in fitting the π–p elastic slope.

In this paper we attempt to properly treat non-identical particles and the s-dependence of σ_{tot}. We now assume that when two high energy particles i and j approach each other the "interaction probability density" ρ_{ij} for elastic scattering is proportional to the product of the densities of "stuff" in each of the two particles. This ρ_{ij} is analogous to a potential, but is formally defined by the fact that its Fourier transform is the elastic scattering amplitude:

$$\left.\frac{\mathrm{d}\sigma}{\mathrm{d}t}\right)^{ij} \bigg/ \left.\frac{\mathrm{d}\sigma}{\mathrm{d}t}\right)^{ij}_0 = |f_{ij}|^2 = \left|\int \mathrm{d}^3\boldsymbol{P}\, \exp\{i\boldsymbol{P}\cdot\boldsymbol{R}\}\, \rho_{ij}(\boldsymbol{R})\right|^2 . \quad (2)$$

In our earlier papers we considered only ρ_{ij} itself and did not try to relate it to the densities of the individual particles. However, Yang et al. [20] have proposed that strong interactions are proportional to the product of the "stuff" of the two incident particles. We find such a product relation quite necessary to study the case of unlike particles. We therefore define a structure function $\varphi_i(\boldsymbol{R}')$ which describes the distribution of stuff in each particle as a function of $\boldsymbol{R}'$ the distance from the center of the particle.

The interaction probability density depends on $\boldsymbol{R}$, the distance between the two incident particles at the instant they scatter. Note that the perpendicular component of $\boldsymbol{R}$ is $R_\perp$ the impact parameter. To obtain the proper dependenc of ρ on $\boldsymbol{R}$ we must fold together $\varphi_i(\boldsymbol{R}')$ and $\varphi_j(\boldsymbol{R}')$; not just multiply them. Thus $\rho_{ij}(\boldsymbol{R})$ is the convolution of the two functions

$$\rho_{ij}(\boldsymbol{R}) = \int \mathrm{d}^3R'\, \varphi_i(\boldsymbol{R}' - \tfrac{1}{2}\boldsymbol{R})\, \varphi_j(\boldsymbol{R}' + \tfrac{1}{2}\boldsymbol{R}) . \quad (3)$$

Now we consider the functions φ_i which describe the particles. When i and j approach each other, each appears to be squashed down by the Lorentz-contraction when viewed from the c.m. frame. However the less massive particle will be squashed down more because of its larger γ-factor.

$$\gamma_i\beta_i = P_{\mathrm{cm}}/M_i\,; \qquad \gamma_j\beta_j = P_{\mathrm{cm}}/M_j\,. \quad (4)$$

The particles might also have different characteristic sizes A_i and A_j. We assume that the particles are spherically symmetric except for the Lorentz-contraction. Finally we assume φ_i is Gaussian in $\boldsymbol{R}'$; while this is independent of the other assumptions it simplifies calculations and apparently agrees with experiment. Thus we have assumed that

$$\varphi_i(\boldsymbol{R}') = \frac{\gamma_i}{(\pi A_i^2)^{3/2}} \exp\left\{-\frac{1}{A_i^2}(X'^2 + Y'^2 + Z'^2\gamma_i^2)\right\} . \quad (5)$$

The normalization was chosen so that

$$\int \mathrm{d}^3R'\, \varphi_i(\boldsymbol{R}') = 1 . \quad (6)$$

This results in dimensionless cross sections and thus only give information about the slope, which is what we want.

We obtain the interaction probability density by substituting eq. (5) for the structure functions φ into eq. (3):

$$\begin{aligned}\rho_{ij}(\boldsymbol{R}) = {}& \frac{\gamma_i\gamma_j}{(\pi A_i A_j)^3} \int \mathrm{d}X'\mathrm{d}Y'\mathrm{d}Z' \\ & \times \exp\left\{-\frac{1}{A_i^2}\left[\left(X' - \frac{X}{2}\right)^2 + \left(Y' - \frac{Y}{2}\right)^2 + \gamma_i^2\left(Z' - \frac{Z}{2}\right)^2\right]\right\} \\ & \times \exp\left\{-\frac{1}{A_j^2}\left[\left(X' + \frac{X}{2}\right)^2 + \left(Y' + \frac{Y}{2}\right)^2 + \gamma_j^2\left(Z' + \frac{Z}{2}\right)^2\right]\right\}\end{aligned} \quad (7)$$

This integral can be done exactly and the result is

$$\rho_{ij}(R)=\frac{\exp\left\{-\left[\frac{X^2+Y^2}{A_i^2+A_j^2}+\frac{Z^2}{A_i^2/\gamma_i^2+A_j^2/\gamma_j^2}\right]\right\}}{\pi^{3/2}(A_i^2+A_j^2)(A_i^2/\gamma_i^2+A_j^2/\gamma_j^2)^{3/2}}\,. \tag{8}$$

The elastic scattering amplitude is the Fourier transform of ρ_{ij} as stated in eq. (2). Taking the Fourier transform of eq. (8) gives

$$f_{ij}(P)=\exp\{-\tfrac{1}{4}[(A_i^2+A_j^2)P_\perp^2+(A_i^2/\gamma_i^2+A_j^2/\gamma_j^2)P_\parallel^2]\}\,. \tag{9}$$

Now for elastic scattering conservation of momentum implies that

$$P_\parallel^2=P_{\rm cm}^2-P_\perp^2\,. \tag{10}$$

Therefore $f_{ij}(P)$ can be rewritten as

$$f_{ij}(P)=\exp\left\{-\tfrac{1}{4}\left[\left\{A_i^2\left(1-\frac{1}{\gamma_i^2}\right)+A_j^2\left(1-\frac{1}{\gamma_j^2}\right)\right\}P_\perp^2\right.\right.$$
$$\left.\left.+\{A_i^2/\gamma_i^2+A_j^2/\gamma_j^2\}P_{\rm cm}^2\right]\right\}. \tag{11}$$

To simplify this we define the parameters

$$(A\beta_{\rm eff})_{ij}^2=\tfrac{1}{2}[A_i^2(1-1/\gamma_i^2)+A_j^2(1-\gamma_j^2)]=$$
$$=\tfrac{1}{2}[A_i^2\beta_i^2+A_j^2\beta_j^2]\,,$$
$$(A/\gamma_{\rm eff})_{ij}^2=\tfrac{1}{2}[A_i^2/\gamma_i^2+A_j^2/\gamma_j^2]\,. \tag{12}$$

Then the elastic scattering amplitude is

$$f_{ij}(P)=\exp\left\{-\tfrac{1}{2}\left[(A\beta_{\rm eff})_{ij}^2P_\perp^2+\left(\frac{A}{\gamma_{\rm eff}}\right)_{ij}^2P_{\rm cm}^2\right]\right\}. \tag{13}$$

Since $P_{\rm cm}=\gamma_i\beta_iM_i=\gamma_j\beta_jM_j$ the second term in the exponent is equal to

$$(A/\gamma_{\rm eff})_{ij}^2P_{\rm cm}^2=[A_i^2\beta_i^2M_i^2+A_j^2\beta_j^2M_j^2]\,. \tag{14}$$

In the high energy limit this approaches the constant $[A_i^2M_i^2+A_j^2M_j^2]$; but in any case this term certainly has no angular dependence so it can be absorbed* into $\mathrm{d}\sigma/\mathrm{d}t)_0$. Then the differential elastic cross section is

$$\left.\frac{\mathrm{d}\sigma}{\mathrm{d}t}\right)^{ij}=\left.\frac{\mathrm{d}\sigma}{\mathrm{d}t}\right)_0^{ij}\exp\{-\tfrac{1}{2}[A_i^2\beta_i^2+A_j\beta_j^2]\,P_\perp^2\}\,. \tag{15}$$

Notice that for p–p scattering $A_i\beta_i=A_j\beta_j$ so that eq. (15) reduces to

$$\left.\frac{\mathrm{d}\sigma}{\mathrm{d}t}\right)^{ij}=\left.\frac{\mathrm{d}\sigma}{\mathrm{d}t}\right)_0^{ij}\exp(-A^2\beta^2P_\perp^2)\,, \tag{16}$$

which was so successful in fitting the ISR data.

Next we consider the effect of the s-dependence of $\sigma_{\rm tot}$ on the elastic slope. Since elastic scattering is the diffraction scattering caused by the inelastic scattering, both types of scattering must occur in a Gaussian region of a fixed size** and shape. Therefore any s-dependence in $\sigma_{\rm tot}$ may indicate an s-dependence in the size of the scattering region which will cause an equivalent s-dependence in the slope b. The slope and $\sigma_{\rm tot}$ are both proportional to the A_i^2:

$$\sigma_{\rm tot}^{ij}(s)=K_{ij}\pi[A_i^2(s)+A_j^2(s)]\,,$$
$$b_{ij}(s)=\tfrac{1}{2}[A_i^2(s)\beta_i^2+A_j^2(s)\beta_j^2]\,. \tag{17}$$

We assume that K_{ij}, the opacity factor, is independent of energy; this implies that the decrease in $\sigma_{\rm tot}^{ij}$ comes from a decrease in A_i and A_j, which seems reasonable in a geometrical model. The s-dependence of the sum of $A_i^2(s)$ and $A_j^2(s)$ is clearly

$$A_i^2(s)+A_j^2(s)=(A_i^2+A_j^2)\,\sigma_{\rm tot}^{ij}(s)/\sigma_{\rm tot}^{ij}(\infty) \tag{18}$$

where A_i^2 and A_j^2 are the sizes at $s=\infty$. However we need the s-dependence of $A_i^2(s)$ and $A_j^2(s)$ separately and we obtain this by the simplest assumption: both have the same s-dependence***

$$A_i^2(s)=A_i^2\,\frac{\sigma_{\rm tot}^{ij}(s)}{\sigma_{\rm tot}^{ij}(\infty)}\,,\qquad A_j^2(s)=A_j^2\,\frac{\sigma_{\rm tot}^{ij}(s)}{\sigma_{\rm tot}^{ij}(\infty)}\,. \tag{19}$$

Substituting this into eqs. (17) we obtain the overall s-dependence of b_{ij}

* This $A^2\beta^2M^2$ term may cone from the fact that our model is 3-dimensional; in ref. [8] we used a 4-dimensional model and the T term exactly cancelled the $A^2\beta^2M^2$ term. However, as stated above, we are only studying the s-dependence of the slope of the cross section and ignoring the s-dependence of its magnitude, so we will not stress this point.

** The characteristic sizes may be different by $\sqrt{2}$ for elastic and inelastic scattering, but the shapes will be the same and the $\sqrt{2}$ is s-independent.

*** Notice that for two different reactions such as π–p and K–p $A_{\rm p}^2(s)$ will have two different s-dependences given by $\sigma_{\rm tot}^{\pi-\rm p}(s)$ and $\sigma_{\rm tot}^{\rm K-p}(s)$, but its value at ∞, $A_{\rm p}^2=10.5$ [GeV/c]$^{-2}$, will be the same for both.

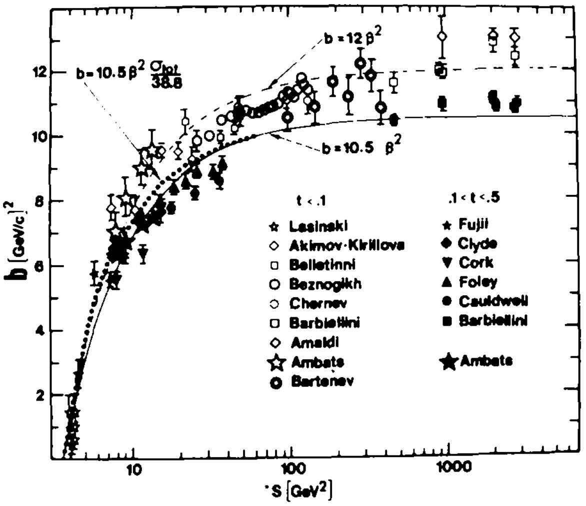

Fig. 1. The slope b plotted against s for p–p elastic scattering. The different data points are identified [1, 18, 21]. Because of the forward peak the data are divided into two t-regions and two curves are shown: solid $b = 10.5\beta^2$ [$t < 0.1$(GeV/c)^2] and dashed $b = 12\beta^2$ [$0.1 < t < 0.5$(GeV/c)^2]. For the large t region eq. (22) is shown as the dotted line which is very similar to $b = 10.5\beta^2$ since σ_{tot} is rather s-independent.

$$b_{ij}(s) = \tfrac{1}{2}\left[A_i^2\beta_i^2 + A_j^2\beta_j^2\right]\, \sigma_{\mathrm{tot}}^{ij}(s)/\sigma_{\mathrm{tot}}^{ij}(\infty)\,. \tag{20}$$

This formula is our central result and gives the s-dependence of the slope of the elastic diffraction peak for all reactions.

Using the experimental [21] values of $\sigma_{\mathrm{tot}}^{ij}(s)$ and 3 parameters

$$A_\pi^2 = 6.1\,, \qquad A_{\mathrm{K}}^2 = 3.3 \quad \text{and} \quad A_{\mathrm{p}}^2 = 10.5\,[\mathrm{GeV}/c]^{-2}\,. \tag{21}$$

Eq. (20) gives the s-dependence of the slope for p–p, $\bar{\mathrm{p}}$–p, $\mathrm{K}^\pm$p, K^-–p, and $\pi^\pm$–p elastic scattering:

$$b_{\mathrm{p}^\pm\mathrm{p}} = 10.5\,\beta_{\mathrm{p}}^2\,\frac{\sigma_{\mathrm{tot}}^{\mathrm{p}^\pm\mathrm{p}}(s)}{38.8}\,,$$

$$b_{\mathrm{K}^\pm\mathrm{p}} = (1.65\beta_{\mathrm{K}}^2 + 5.25\beta_{\mathrm{p}}^2)\,\frac{\sigma_{\mathrm{tot}}^{\mathrm{K}^\pm\mathrm{p}}(s)}{17.5}\,, \tag{22}$$

$$b_{\pi^\pm\mathrm{p}} = (3.05\beta_\pi^2 + 5.25\beta_{\mathrm{p}}^2)\,\frac{\sigma_{\mathrm{tot}}^{\pi^\pm\mathrm{p}}}{24.6}\,.$$

Notice we assumed that $\sigma_{\mathrm{tot}}(\infty)$ is the same for particle and antiparticle scattering. These curves are plotted in fig. 1 through 4 along with the experimental values of b_{ij} taken from various compilations [21]. The fit seems very good. It is especially impressive that there are only 3 parameters and that there are no free parameters to distinguish p–p from $\bar{\mathrm{p}}$–p or K^+–p from K^-–p. The experimental differences in σ_{tot} thus seem to account for the differences in these slopes. Below 3 GeV/c the fit is not good and this is because at low energies the scattering is no longer diffractive, and geometrical models are less useful.

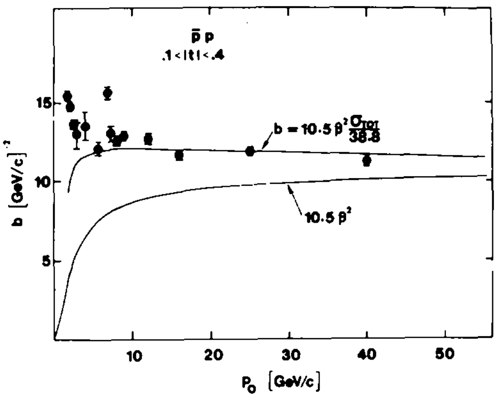

Fig. 2. Slope b plotted against P_0(Lab) for $\bar{\mathrm{p}}$–p elastic scattering. The data points are shown [21]. Eq. (22) is shown along with the curve $10.5\beta^2$ to show the importance of $\sigma_{\mathrm{tot}}(s)$ for $\bar{\mathrm{p}}$–p.

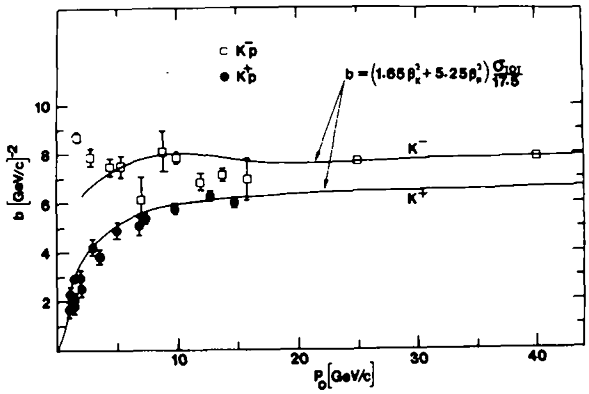

Fig. 3. Slope b plotted against P_0(Lab) for $\mathrm{K}^\pm$–p elastic scattering. The data points are shown [21]. Eq. (22) is shown for the two cases. The entire difference is due to the differences in σ_{tot} for K^+–p and K^-–p.

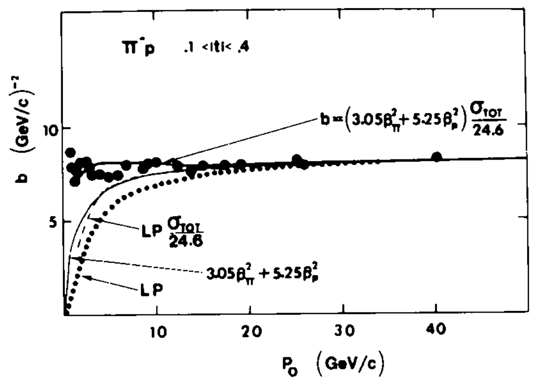

Fig. 4. Slope b plotted against P_0(Lab) for π^-–p elastic scattering. The data points are shown [21]. Eq. (22) (thick line) is shown along with $b = 3.05\beta_\pi^2 + 5.25\beta_p^2$ (thin line) to show the effect of $\sigma_{tot}(s)$. The Leader and Pennington fit [13] is shown as a dotted line and their fit modified by $\sigma_{tot}(s)/\sigma_{tot}(\infty)$ is shown as a dashed line.

For π^-–p scattering the n^2 fit of Leader and Pennington is shown as a dotted line in fig. 4. Their fit is somewhat improved by multiplying by $\sigma_{tot}/\sigma_{tot}(\infty)$ as shown by the dashed line. However the fit is still marginal and the use of $\sigma_{tot}/\sigma_{tot}(\infty)$ is not very natural in a group theoretical model. For p–p scattering $n^2 = \beta^2 P_\perp^2$; and n^2 and eqs. (22) are rather similar for K^+–p scattering. However for K^-–p and $\bar{p}$–p scattering the geometrical model seems to give a better fit.

In summary this Lorentz contracted geometrical model seems to fit the s-dependence of the slope of the elastic diffraction peak for many reactions with only 3 parameters and the experimental σ_{tot}.

I would like to thank Professor M.H. Ross for many discussions and Dr. R. Diebold for his comments.

References

[1] U. Amaldi et al., Phys. Lett. 36B (1971) 504;
M. Holder et al., Phys. Lett. 35B (1971) 351; 35B (1971) 361;
G. Barbiellini et al., Phys. Lett. 39B (1972) 663.
[2] L.G. Ratner et al., Phys. Rev. Lett. 27 (1971) 68; Proc. 1971 Rochester Conf. of APS, (1971) p. 99;
J.C. Sens, Rapporteur talk at 1972 Oxford Conf.
[3] R. Serber, Phys. Rev. Lett. 10 (1963) 357; Rev. Mod. Phys. 36 (1964) 649.
[4] A.D. Krisch, Phys. Rev. Lett. 11 (1963) 217.
[5] L. Van Hove, Nuovo Cimento 28 (1963) 798.
[6] T.T. Wu and C.N. Yang, Phys. Rev. 137 (1965) B708.
[7] A.D. Krisch, Phys. Rev. 135 (1964) B1456.
[8] A.D. Krisch, Lectures in theoretical physics, Vol. IX, eds. W.E. Britten et al., (Univ. of Colorado Press, Boulder, Colorado, 1966) p. 1; Phys. Rev. Lett. 19 (1967) 1149.
[9] A.D. Krisch, Proc. of McGill University - Canada Institute of Particle Physics Summer School, 1972, to be published.
[10] K. Huang, Phys. Rev. 156 (1967) 1555.
[11] C.N. Yang et al., Phys. Rev. 188 (1969) 2159; Phys. Rev. Lett. 25 (1970) 1072.
[12] R.P. Feynman, Phys. Rev. Lett. 23 (1969) 1415; and private communication.
[13] E. Leader and M.R. Pennington, Phys. Rev. Lett. 27 (1971) 1325; and later preprint.
[14] S. Barshay and Y.A. Chao, Phys. Lett. 38B (1972) 225; 229;
J.S. Ball and S.S. Pinsky, Phys. Rev, Lett. 27 (1972) 1820.
[15] J. Allaby et al., CERN Topical Conf. on High energy collisions of hadrons, CERN 68-7 (1968) p. 580.
[16] R.A. Carringan et al., Phys. Rev. Lett. 24 (1970) 683.
[17] G. Barbiellini et al., XVI Intern. Conf. on High energy physics, Chicago (1972).
[18] V. Bartenev et al., XVI Intern. Conf. on High energy physics, Chicago (1972).
[19] This arbitrariness was stressed by M.H. Ross, private communication (1965).
[20] T.T. Chou and C.N. Yang, Phys. Rev. Lett. 20 (1968) 1213;
N. Beyers and C.N. Yang, Phys. Rev. 142 (1966) 976.
[21] G.G. Bezogikh et al., Phys. Lett. 30B (1969) 274;
I. Ambats et al., Phys. Rev. Lett. 29 (1972) 1415;
T. Lasinski et al., Phys. Rev. 179 (1969) 1426;
Particle Data Group Compilations: UCRL - 20000NN, UCRL - 20000K⁺N, UCRL - 20000 p̄p;
G. Giacomelli, CERN-HERA 69-3;
A.N. Diddens, Total and elastic cross sections, Proc. 1972 Oxford Conf.